Synthesis and Characterization of Novel Self-Generating Liquid MOCVD Precursors for Thin Films of Zinc Oxide

Antonino Gulino,*,† Francesco Castelli,† Paolo Dapporto,‡ Patrizia Rossi,‡ and Ignazio Fragalà*,†

Dipartimento di Scienze Chimiche, Università di Catania, Viale Andrea Doria 6, 95125 Catania, Italy, and Dipartimento di Energetica, Università di Firenze, Via Santa Marta 3, 50139 Firenze, Italy

Received October 8, 1999. Revised Manuscript Received December 8, 1999

Three novel $Zn(hfa)_2 \cdot 2H_2O \cdot$polyether adducts have been prepared through simple procedures with stoichiometric quantities of zinc hydroxide, Hhfa, and polyether. The products have been characterized by elemental analysis, X-ray single-crystal analysis, fast atom bombardment mass spectra, ^1H and ^{19}F NMR spectra, thermogravimetric (TG)−differential TG−differential scanning calorimetry (DSC) thermal measurements, and infrared transmittance spectroscopy. An attempt to obtain water-free adduct was unsuccessful even using excess polyethers. X-ray single-crystal data of the $Zn(hfa)_2 \cdot 2H_2O \cdot$diglyme adduct show that the polyether does not coordinate to the metal center. Nevertheless, metrical data are indicative of bridging interactions involving the oxygen of one coordinated H_2O molecule and the three oxygens of the diglyme. Very mild heating (37−51 °C) results in liquid compounds that, in turn, can easily be evaporated. Preliminary gas-phase Fourier transform-IR measurements in vacuo suggest that the anhydrous $Zn(hfa)_2 \cdot$diglyme forms upon evaporation due to competing H_2O and diglyme ancillary ligation. Deposition experiments, in a low-pressure horizontal hot-wall reactor, on fused SiO_2 (quartz) substrates, result in ZnO films. X-ray diffraction measurements provide evidence that they consist of hexagonal (002) and (10*l*) oriented, crystals. UV−vis spectra show that the transmittance of as deposited films in the visible region is about 90%.

Introduction

ZnO has been thoroughly studied in the perspective of catalytic applications and gas sensing.[1] It adopts the wurtzite structure (space group $P6_3mc$) pictorially described in terms of hexagonal close packing (hcp) of oxygen ions stacked along the [001] direction with cations occupying one-half of the tetrahedral sites.[2,3] It is an intrinsic *n*-type semiconductor having a band gap of ∼3.3 eV[4] due to lattice defects consisting of oxygen vacancies and involving interstitial ($Zn^{2+} - 2e^-$) pairs and cation and anion vacancies ($\square_M$, $\square_O$).[5] The band gap width, in polycrystalline ZnO, shows anomalous behavior because of the existence of potential barriers at the grain boundaries[6,7] whereas the resistivities depend on the synthetic procedure or the presence of dopants within the ZnO lattice.[8−15]

Thin films of ZnO have a large number of important applications in solar cells,[16] surface acoustic wave devices,[17] optical waveguides,[18] varistors,[19,20] gas sensors,[21] photoluminescent devices,[22−24] and as catalysts.[5] They have been grown using a large variety of techniques including sublimation,[25] pulsed laser deposition (PLD),[26] spray pyrolysis (SP),[27,28] atomic layer

* E-mail: lfragala@dipchi.unict.it and agulino@dipchi.unict.it.
† Università di Catania.
‡ Università di Firenze.

(1) Henrich, V. E.; Cox, P. A. *The Surface Science of Metal Oxides*; Cambridge University Press: Cambridge, 1994.
(2) McCoy, M. A.; Grimes, R. W.; Lee, W. E. *J. Mater. Res.* **1996**, *11*, 2009.
(3) Abrahams, S. C.; Bernstein, J. L. *Acta Crystallogr.* **1969**, *B25*, 1233.
(4) Studenikin, S. A.; Golego, N.; Cocivera, M. *J Appl. Phys.* **1998**, *84*, 5001.
(5) Miller, B. J. A.; Maertin-Luengo, M. A.; Vong, M. S. W.; Wang, Y.; Self, V. A.; Chapman, S. M.; Sermon, P. A. *J. Mater. Chem.* **1997**, *7*, 2155.
(6) Roth, A. P.; Webb, J. B.; Williams, D. F. *Phys. Rev. B* **1982**, *25*, 7836.
(7) Srikant, V.; Clark, D. R. *J. Mater. Res.* **1997**, *12*, 1425.
(8) Tang, W.; Cameron, D. C. *Thin Solid Films* **1994**, *238*, 83.
(9) Wang, R.; Sleight, A. W.; Cleary, D. *Chem. Mater.* **1996**, *8*, 433.
(10) Agarwal, G.; Speyer, R. F. *J. Mater. Res.* **1997**, *12*, 2447.
(11) Palmer, G. B.; Poeppelmeier, K. R.; Mason, T. O. *Chem. Mater.* **1997**, *9*, 3121.
(12) Wu, X.; Coutts, T. J.; Mulligan, P. W. *J. Vac. Sci. Technol. A* **1997**, *15*, 1057.
(13) Djembo-Taty, K.; Plaindoux, L.; Kossanyi, J.; Ronfard-Haret, J. C. *J. Chim. Phys.* **1998**, 95, 595.
(14) Kazeoka, M.; Hiramatsu, H.; Seo, W.; Koumoto, K. *J Mater. Res.* **1998**, *13*, 523.
(15) Tsubota, T.; Ohtaki, M.; Eguchi, K.; Arai H. *J. Mater. Chem.* **1998**, *8*, 409.
(16) Chopra, K. L.; Das, S. R. *Thin Film Solar Cells*; Plenum: New York, 1983.
(17) Shih W.-C.; Wu, M.-S. *J. Cryst. Growth* **1994**, *137*, 319.
(18) Ohtomo, A.; Kawasaki, M.; Koida, T.; Masubuchi, K.; Koinuma, H.; Sakurai, Y.; Yoshida, Y.; Yasuda, T.: Segawa, Y. *Appl. Phys. Lett.* **1998**, *72*, 2466.
(19) Lin, F.-C.; Takao, Y.; Shimizu, Y.: Egashira, M. *Sens. Actuators, B* **1995**, *24−25*, 843.
(20) Ramanchalam, M. S.; Rohatgi, A.; Carter, W. B.; Shaffer, J. P.: Gupta, T. K. *J. Electron. Mater.* **1995**, *24*, 413.
(21) Weissenrieder, K. S.: Muller, J. *Thin Solid Films* **1997**, *300*, 30.
(22) Studenikin, S. A.; Golego, N.; Cocivera, M. *J Appl. Phys.* **1998**, *84*, 2287.
(23) Dahan, P.; Fleurov, V.; Thurian, P.; Heitz, R.; Hoffmann, A.; Broser, I. *J. Phys.: Condens. Matter* **1998**, *10*, 2007.
(24) Egelhaaf, H.-J.: Oelkrug, D. *J. Cryst. Growth* **1996**, *161*, 190.

10.1021/cm991154k CCC: $19.00
Published on Web 02/03/2000

deposition (ALD),[29] molecular beam epitaxy (MBE),[30] chemical bath deposition (CBD),[31] sol−gel,[8] electrodeposition,[32,33] thermal decomposition[34,35] oxidation of zinc films,[36] and metal organic chemical vapor deposition (MOCVD).[37−43]

In MOCVD applications, the liquid dimethyl−[43] and diethyl−Zn complexes,[41] as well as the solid acetate−,[37−38,42] alkoxide−,[39] and acetylacetonate−[40] Zn complexes have been used as precursors. In this context, MOCVD from liquid precursors certainly represents an issue of considerable relevance due to the accurate reproducibility associated with constant evaporation (hence constant mass-transport) rates for given source temperatures.

In the present investigation, we report on novel self-generating liquid adducts that, in addition, have proven to be well-suited precursors for MOCVD of ZnO films.

Experimental Details

The $Zn(C_5F_6HO_2)_2{\cdot}2H_2O{\cdot}CH_3(OCH_2CH_2)_2OCH_3$ (**1**), $Zn(C_5F_6HO_2)_2{\cdot}2H_2O{\cdot}CH_3(OCH_2CH_2)_3OCH_3$ (**2**), and $Zn(C_5F_6HO_2)_2{\cdot}2H_2O{\cdot}CH_3(OCH_2CH_2)_4OCH_3$ (**3**) adducts (hereafter, $Zn(hfa)_2{\cdot}2H_2O{\cdot}$diglyme, $Zn(hfa)_2{\cdot}2H_2O{\cdot}$triglyme, and $Zn(hfa)_2{\cdot}2H_2O{\cdot}$tetraglyme, respectively; hfa = 1,1,1,5,5,5-hexafluoro-2,4-pentanedionate ligand, diglyme = bis(2-methoxyethyl)ether, triglyme = 2,5,8,11-tetraoxadodecane, and tetraglyme = 2,5,8,-11,14-pentaoxapentadecane) were synthesized by refluxing a CH_2Cl_2 suspension of stoichiometric quantities of $Zn(OH)_2$, $C_5F_6H_2O_2$ (hereafter H−hfa) and the appropriate polyether. An attempt to obtain water-free adducts proved unsuccessful even when excess of polyethers was added. By contrast, all synthetic approaches to the monoglyme adduct were unsuccessful, and the simple, unadducted $Zn(C_5F_6HO_2)_2{\cdot}2H_2O$ complex was always obtained.

Aldrich grade reagents were used throughout all present syntheses.

The elemental analyses were performed using a Carlo Erba elemental analyzer EA 1108.

Table 1. Crystal Data and Structure Refinement

identification code	$Zn(hfa)_2{\cdot}2H_2O{\cdot}$diglyme
empirical formula	C16 H20 F12 O9 Zn
formula weight	649.69
temperature	293(2) K
wavelength	1.54180 Å
crystal system	triclinic
space group	$P\,{-}1$
unit cell dimensions	$a = 9.139(3)$ Å; $\alpha = 94.52(3)°$ $b = 11.561(2)$ Å; $\beta = 101.21(3)°$ $c = 14.054(5)$ Å; $\gamma = 112.62(2)°$
volume	1325.0(7) Å^3
Z	2
density (calculated)	1.628 g/cm^3
absorption coefficient	2.483 mm^{-1}
$F(000)$	652
crystal size	0.8 × 0.8 × 0.2 mm
Θ range for data collection	3.0 to 65.0°
index ranges	$-10 \le h \le 10$, $-13 \le k \le 13$, $0 \le l \le 16$
reflections collected	4321
independent reflections	4321
refinement method	full-matrix least-squares on F^2
data/parameters	4321/347
goodness-of-fit on F^2	1.052
final R indices [$I > 2$sigma(I)]	$R_1 = 0.0642$, w$R_2 = 0.1676$
R indices (all data)	$R_1 = 0.0654$, w$R_2 = 0.1692$
extinction coefficient	0.0000(5)
largest diff. peak and hole	1.117 and −0.748 e Å^{-3}

FAB mass spectra were obtained using a Kratos MS 50 spectrometer.

^{1}H and ^{19}F NMR spectra were recorded using a Varian 500 MHz spectrometer.

The thermal behavior of the $Zn(hfa)_2{\cdot}2H_2O{\cdot}$polyether adducts was investigated by thermal (TGA), differential gravimetric analysis (DTG), and differential scanning calorimetry (DSC), under prepurified nitrogen, using a 1 °C/min heating rate. A Mettler TA 4000 system equipped with a DSC-30 cell, a TG 50 thermobalance, and a TC 11 processor was used.[44,45] Samples (5−6 mg) were accurately weighed and examined in the 10−400 °C range. The sensitivity was 1.72 mW.

Infrared transmittance spectra were recorded using a Jasco FT/IR-430 spectrometer. The instrumental resolution was 2 cm^{-1}.

Crystal data and refinement details of the structure of $Zn(hfa)_2{\cdot}2H_2O{\cdot}$diglyme are reported in Table 1. Unit cell parameters and intensity data were obtained on a Siemens P4 diffractometer. Cell dimensions were determined by least-squares fitting of 25 centered reflections. Three standard reflections were measured to check the stabilities of the crystal and the diffractometer. The intensity data were corrected for a slow and continuous loss of intensity detected during the collection. Data were then corrected for Lorentz and polarization effects, and an absorption correction was applied using the analytical method based on the measure of the indexed faces of the crystal used and on direction cosines of the reflections. The structure was solved by direct methods, using SIR-97 program[46] and subsequently refined on the F^2 values by the full-matrix least-squares program SHELXL-93[47] using all reflections. The hydrogen atoms linked to the carbon atoms of the hfa ligand and the diglyme molecule were introduced in calculated positions, and their positions were refined according to the attached carbon atom. The hydrogen atoms of the water molecules were not found in the ΔF Fourier synthesis and were not introduced in the calculations. The

(25) Ntep, J.-M.; Barbé, M.; Cohen-Solal, G.; Bailly, F.; Lusson, A.; Triboulet, R. *J. Cryst. Growth* **1998**, *184/185*, 1026.
(26) Vispute, R. D.; Talyansky, V.; Choopun, S.; Sharma, R. P.; Venkatesan, T.; He, M.; Tang, X.; Halpern, J. B.; Spencer, M. G.; Li, Y. X.; Salamanca-Riba, L. G.; Iliadis, A. A.: Jones, K. A. *Appl. Phys. Lett*. **1998**, *73*, 348.
(27) Fiddes, A. J. C.; Durose, K.; Brinkman, A. W.; Woods, J.; Coates, P. D.; Banister, A. J. *J. Cryst. Growth* **1996**, *159*, 210.
(28) Benramdane, N.; Murad, W. A.; Misho, R. H.; Ziane, M.; Kebbab, Z. *Mater. Chem. Phys*. **1997**, *48*, 119.
(29) Yamada, A.; Sang, B.: Konagai, M. *Appl. Surf. Sci*. **1997**, *112*, 216.
(30) Tang, Z. K.; Wong, G. K. L.; Yu, P.; Kavasaki, M.; Ohtomo, A.; Koinuma, H.; Segawa, Y. *Appl. Phys. Lett*. **1998**, *72*, 3270.
(31) O'Brien, P.; Saeed, T.; Knowles, J. *J. Mater. Chem*. **1996**, *6*, 1135.
(32) Nyffenegger, R. M.; Craft, B.; Shaaban, M.; Gorer, S.; Erley, G.; Penner, R. M. *Chem. Mater*. **1998**, *10*, 1120.
(33) Peulon, S.; Lincot, D. *Adv. Mater*. **1996**, *8*, 166.
(34) Audebrand, N.; Auffrédic, J. P.; Louër, D. *Chem. Mater*. **1998**, *10*, 2450.
(35) Baird, T.; Campbell, K. C.; Holliman, P. J.; Hoyle, R. W.; Stirling, D.; Williams, B. P.; Morris, M. *J. Mater. Chem*. **1997**, *7*, 319.
(36) Kashani, H. *J. Mater. Sci.: Mater. Electron*. **1996**, *7*, 85.
(37) Jain, S.; Kodas, T. T.; Hampden-Smith, M. *Chem. Vap. Deposition* **1998**, *4*, 51.
(38) Mar, G. L.; Timbrell P. Y.; Lamnb, R. N. *Chem. Mater*. **1995**, *7*, 1890.
(39) Auld, J.; Houlton, D. J.; Jones, A. C.; Rushworth, S. A.; Malik, M. A.; O'Brien, P.; Critchlow, G. W. *J. Mater. Chem*. **1994**, *4*, 1249.
(40) Sato, H.; Minami, T.; Miyata, T.; Takata, S.; Ishii, M. *Thin Solid Films* **1994**, *246*, 65.
(41) Hu, J.; Gordon, R. *J. Appl. Phys*. **1992**, *71*, 880.
(42) Kim, S. J.; Marzouk, H. A.; Reucroft, P. J.; Hamrin, C. E., Jr. *Thin Solid Films* **1992**, *217*, 133.
(43) Hu, J; Gordon, R. G. *Mater. Res. Soc. Symp. Proc*. **1991**, *202*, 457.
(44) Malandrino, G.; Benelli, C.; Castelli, F.; Fragalà, I. *Chem. Mater*. **1998**, *10*, 3434.
(45) Malandrino, G.; Castelli, F.; Fragalà, I. *Inorg. Chim. Acta* **1994**, *224*, 203.
(46) Altomare, A.; Cascarano, G.; Giacovazzo, C.; Guagliardi, A.; Burla, M. C.; Polidori, G.; Camalli, M. *J. Appl. Crystallogr*. **1994**, *27*, 435.
(47) Sheldrich, G. M. *SHELX 93*, Program for crystal structure determination, University Of Göttingen, Germany, 1994.

Table 2. MOCVD Conditions

substrate temperature	320−400 °C
total pressure	2−6 Torr
O_2 gas flow rate	100 sccm
Ar gas flow rate	100−200 sccm
source sublimation temperature	60−80 °C
deposition time	120−180 min

carbon, oxygen, fluorine, and zinc atoms were refined anisotropically, whereas for the hydrogen atoms, an overall isotropic temperature factor was calculated and subsequently refined to a final U value of 0.150(6) Å^2. Atomic scattering factors and anomalous dispersion corrections for all the atoms were taken from results collected elsewhere.[48] Geometrical calculations were performed by PARST93.[49] The molecular plot was produced by the ORTEP program.[50]

X-ray diffraction (XRD) powder data were recorded on a Bruker D-5005 diffractometer operating in a $\theta-\theta$ geometry (Cu Kα radiation 30 mA and 40 kV) over a $30° < 2\theta < 70°$ angular range.

XPS measurements were made with a PHI 5600 multitechnique system (base pressure of the main chamber 3×10^{-10} Torr). Resolution, correction for satellite contributions and background removal have been described elsewhere.[51]

MOCVD experiments were performed using an horizontal hot-wall reactor,[52] under reduced pressure, using the present, as synthesized, $Zn(hfa)_2{\cdot}2H_2O{\cdot}$diglyme. Fused SiO_2 (quartz) was used as substrate after cleaning in an ultrasonic bath with isopropyl alcohol. Pure Ar (100−200 sccm) and O_2 (100 sccm) were used as carrier and reaction gases, respectively (Table 2). The total pressure, kept in the 2−6 Torr range, was measured using a MKS Baratron 122AAX system. Flow rates were controlled within ±2 sccm using MKS flow controllers and a MKS 147 multigas controller.

Synthesis of $Zn(hfa)_2{\cdot}2H_2O{\cdot}$diglyme (1). The $Zn(hfa)_2{\cdot}2H_2O{\cdot}$diglyme adduct was synthesized by adding, under vigorous stirring, 0.497 g (0.005 mol) of $Zn(OH)_2$, 1.41 mL (0.01 mol) of H−hfa, and 0.72 mL of diglyme (0.005 mol) to 60 mL of CH_2Cl_2. The resulting suspension was refluxed under stirring for 1 h. After a few minutes refluxing, the suspension became clear. No excess $Zn(OH)_2$ was filtered off. A colorless oil was obtained after evaporation of the CH_2Cl_2 solvent. A white powder was obtained after adding the resulting oils to 30 mL of pentane or hexane, whereas colorless crystals resulted by dissolving the oil in 90 mL of pentane or hexane and leaving the solution to concentrate to room temperature. Yield: 88%. A similar synthetic procedure carried out with ZnO instead of $Zn(OH)_2$ gave no significant yield. This behavior has been previously reported also for the synthesis of $Zn(hfa)_2$.[53] $Zn(OH)_2$ was, therefore, freshly prepared by the dropwise addition of a saturated $NaHCO_3$ solution to ZnO dissolved in a dilute HCl solution. The hydroxide gel thus formed was filtered off, washed with distilled water, and dried at room temperature. Mp (crude product): 37−38 °C. Elem. Anal. for $ZnC_{16}H_{20}F_{12}O_9$: C = 29.63; H = 3.09. Found: C = 29.65; H = 3.04%. MS (FAB$^+$, 70 eV, *m/e* fragments; M* = $Zn(hfa)_2{\cdot}$diglyme): 661 (M* + CF_2)$^+$, 497 (M* − diglyme + F)$^+$, 424 (M* − hfa + F)$^+$, 409 (M* − diglyme − CF_3)$^+$, 405 (M* − hfa)$^+$, 362 (M* − hfa − CH_2CH_2O)$^+$, 290 (M* − diglyme − hfa + F)$^+$. IR (Nujol; ν/cm^{-1}): 3450 (s), 3260 (s), 1650 (s), 1613 (vw), 1555 (m), 1529 (m), 1514 (w), 1352 (w), 1256 (s), 1201 (s), 1148 (s), 1110 (m), 1086 (m), 1020 (m), 947 (w), 863 (m), 839 (m), 807 (w), 793 (m), 757 (vw), 740 (w), 667 (s). ^{1}H NMR ($CDCl_3$): δ 6.07 (s, 2H); 3.79−3.77 (t 4H), 3.62−3.60 (t 4H), 3.40 (s 6 H), 1.90 (s 4H). ^{19}F NMR:-1.908($CDCl_3$) (s, 12H).

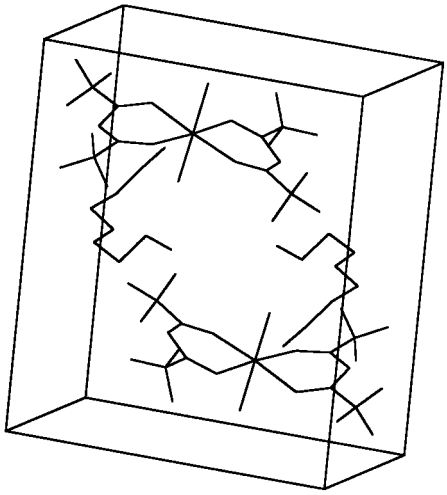

Figure 1. ORTEP drawing of one of the two molecules present in the unit cell of $Zn(hfa)_2{\cdot}2H_2O{\cdot}$diglyme.

Synthesis of $Zn(hfa)_2{\cdot}2H_2O{\cdot}$triglyme (2). A similar synthetic approach was adopted for the triglyme adduct using 0.497 g (0.005 mol) of $Zn(OH)_2$, 1.41 mL (0.01 mol) of H−hfa, and 0.9 mL of triglyme (0.005 mol) to 60 mL of CH_2Cl_2. Yield: 86%. Mp (crude product): 49−50 °C. Elem. Anal. for $ZnC_{18}H_{24}F_{12}O_{10}$: C = 31.16; H = 3.49. Found: C = 31.20; H = 3.24%. IR (Nujol; ν/cm^{-1}): 3378 (s), 3267 (s), 1655 (s), 1616 (w), 1553 (m), 1533 (s), 1516 (m), 1348 (m), 1256 (s), 1193 (s), 1147 (s), 1107 (s), 1090 (m), 1018 (s), 942 (s), 864 (sh), 844 (s), 808 (m), 791 (s), 757 (m), 741 (w), 668 (s). ^{1}H NMR ($CDCl_3$): δ 6.06 (s, 2H), 3.74−3.72 (quartet 8H), 3.64−3.62 (partially overlapped dq. 4H), 3.41 (s 6 H), 1.66 (s 4H).

Synthesis of $Zn(hfa)_2{\cdot}2H_2O{\cdot}$tetraglyme (3). The synthesis procedure was similarly adopted to **3** using 0.497 g (0.005 mol) of $Zn(OH)_2$, 1.41 mL (0.01 mol) of H−hfa, and 1.1 mL of tetraglyme (0.005 mol) to 60 mL of CH_2Cl_2. Yield: 84%. Mp (crude products): 50−51 °C. Elem. Anal. for $ZnC_{20}H_{28}F_{12}O_{11}$: C = 32.56; H = 3.82. Found: C = 32.62; H = 3.82%. IR (Nujol; ν/cm^{-1}): 3375 (s), 3263 (s), 1650 (s), 1614 (vw), 1553 (m), 1529 (m), 1513 (w), 1255 (s), 1198 (s), 1147 (s), 1120 (m), 1093 (m), 1022 (m), 945 (m), 860 (w), 842 (m), 808 (w), 789 (m), 758 (m), 740 (w), 668 (s). ^{1}H NMR ($CDCl_3$): δ 6.04 (s, 2H); 3.73−3.71 (quint. 8H); 3.69−3.67 (quart. 4H); 3.62−3.61 (quart. 4H), 3.40 (s 6 H), 1.90 (s 4H).

Results and Discussion

The $Zn(hfa)_2{\cdot}2H_2O{\cdot}$diglyme complex crystallizes in the triclinic space group P-1 with two units in a cell of dimension a = 9.139(3) Å, b = 11.561(2) Å, c = 14.054(5) Å, α = 94.52(3)°, β = 101.21(3)°, and γ = 112.62(2)°. The structure was refined to a final R factor of 0.0642 based on 4321 independent reflections. A view of the complex is given in Figure 1 and the packing in the cell is depicted in Figure 2.

The octahedral coordination around the Zn atom is fairly regular. The ZnO bond distances range from 2.050 (Zn(1)−O(1)) to 2.122 Å (Zn(1)−O(5)) and can be grouped in two lists of three values each: (i) those represented by Zn(1)−O(1) = 2.050(2) Å, Zn(1)−O(3) = 2.061(2) Å, and Zn(1)−O(6) = 2.066(2) Å and (ii) those, somewhat larger, represented by Zn(1)−O(2) = 2.093(2) Å, Zn(1)−O(4) = 2.100(2) Å, and Zn(1)−O(5) = 2.122(2) Å. The ligand geometry is normal with the partial double bonds C(1)−C(2) = 1.386(5) Å and C(2)−C(3) = 1.387(5) Å having similar bond lengths, whereas the nominal single C(1)−C(4) and C(3)−C(5) are 1.527(5) Å and 1.536(5)

(48) *International Tables for X-ray Crystallography*, Kynoch Press: Birmingham, U.K., 1974; Vol. 4, .
(49) Nardelli, M. *Comput. Chem.* **1983**, *7*, 95.
(50) Johnson, C. K. *ORTEP, Rep. ORNL 3794*; Oak Ridge National Laboratory, TN, 1971.
(51) Gulino, A.; La Delfa, S.; Fragalà, I.; Egdell, R. G. *Chem. Mater.* **1996**, *8*, 1287.
(52) Gulino, A.; Compagnini, G.; Egdell, R. G.; Fragalà, *I. Thin Solid Films* **1999**, in press.
(53) Chattoraj, S. C.; Cupka, A. G., Jr.; Sievers, R. E. *J. Inorg. Nucl. Chem.* **1996**, *28*, 1937.

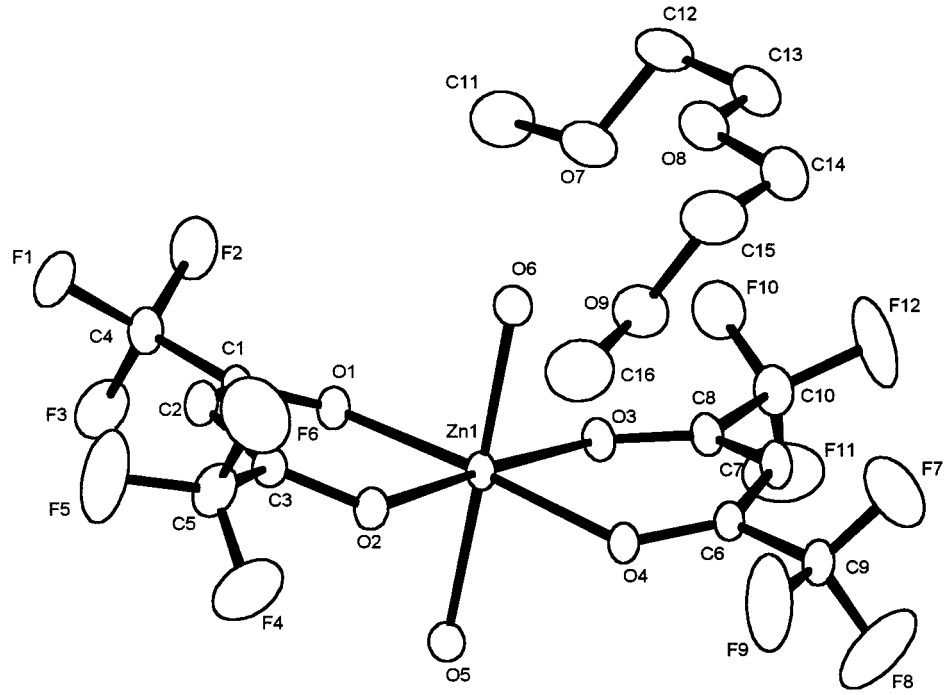

Figure 2. Packing cell of the $Zn(hfa)_2 \cdot 2H_2O \cdot$diglyme.

Å, respectively. The C(1)−O(1) and C(3)−O(2) bonds are 1.242(4) and 1.248(4) Å, respectively, and are also indicative of the aromatic character of the ligand.

The Zn atom lies in the plane defined by the positions of the four oxygen atoms of the two β-carbonyl groups, being marginally displaced (0.0189(4) Å) toward the water molecule with the oxygen O(6). The angular distortions from idealized octahedral symmetry around the Zn are very small, the trans angles being 175.84 (7)° O(3)−Zn(1)−O(2), 175.88(7)° O(1)−Zn(1)−O(4)° and 178.85(7)° O(6)−Zn(1)−O(5). Moreover, the O(1)−Zn(1)−O(3) angle of 96.28(9)° is larger than the others, O(1)−Zn(1)−O(2) = 87.87(9)°, O(2)−Zn(1)−O(4) = 88.42 (9)°, and O(3)−Zn(1)−O(4) = 87.42(9)°. The angles O(5−6)−Zn(1)−O(1−4) fall in the 88.84(9)− 91.48(10)° range.

The temperature factors of the fluorine atoms are rather large and cause some disorder. The diglyme molecule does not coordinate to the metal, even though it interacts with the water O(6) atom. In fact, the short contacts involving the diglyme oxygens and the water oxygen, O(6)···O(7) = 2.717(3), O(6)···O(8) = 3.029(6), and O(6)···O(9) = 2.732(5) Å, are indicative of bridging hydrogen bonds. Unfortunately, the hydrogen atoms of the two water molecules have not been found in the ΔF Fourier, thus precluding any quantitative further discussion of the hydrogen bonding.

The remainder water molecule (marked by the O(5)) forms intermolecular contacts with some fluorine atoms of the β-carbonyl groups: O(5)···F(4) = 3.237(5) and O(5)···F(9) = 3.224(7) Å.

The geometric conformation of the polyether, conditioned by the presence of bridged hydrogen bonds involving the water molecule, becomes clear from the ORTEP drawing in Figure 1. The two dihedral angles around the C(12)−C(13) and C(14)−C(15) bonds (−65.1 (7)° and 65.5(8)°, respectively), are indicative of a gauche conformation. These angles are an obvious consequence of contact interactions of all of the three oxygen diglyme atoms with the water molecule O(6) bonded to the Zn center.

It has been previously reported that orthorhombic crystals of the trans $Zn(hfa)_2 \cdot 2H_2O$ complex contain solvent water molecules that cause oligomerization by extensive hydrogen bonds[54] and suggest the $[Zn(hfa)_2 \cdot (H_2O)_2] \cdot H_2O$ formulation. In the case of the present adduct **1**, the diglyme solvation plays an identical role and present metrical data are entirely comparable with those already reported for the trans $[Zn(hfa)_2 \cdot (H_2O)_2] \cdot H_2O$.[54]

The MS−FAB spectra of the prototypical $Zn(hfa)_2 \cdot 2H_2O \cdot$diglyme do not show the molecular ion peak. The observed peaks always show the characteristic isotope pattern of Zn and are due to the loss of the hfa and polyether fragments. In addition, there is evidence of fluorine or CF_2 group transfer processes similar to that observed in closely related adducts.[44,55] The most intense peak at 424 *m/e* (100%) corresponds to the fragment $[M^* - hfa + F]^+$. At lower mass, the most significant peaks at 405 *m/e* (78%) and 290 *m/e* (92%) can be associated with the $[M^* - hfa]^+$ and $[M^* - hfa -$ diglyme $+ F]^+$ fragments, respectively.

The ^1H NMR spectra of the $Zn(hfa)_2 \cdot 2H_2O \cdot$polyether adducts always show a singlet at $\delta = 6.04-607$, whose integration accounts for the two protons of the hfa ring ligands. In addition, multiplets at $\delta = 3.8-3.6$ represent resonances of methylenic protons of polyethers, whereas the singlet at $\delta \approx 3.40$ is consistent with the six protons of the two methyl groups of the same ligands. Finally, the resonance at $\delta = 1.66-1.90$ (four protons) is associated with the two coordinated H_2O molecules. The ^{19}F NMR spectrum of the $Zn(hfa)_2 \cdot 2H_2O \cdot$diglyme shows a singlet resonance at $\delta = -1.908$. Present resonances are

(54) Adams, R. P.; Allen, H. C., Jr.; Rychlewska, U.; Hodgson, D. J. *Inorg. Chim. Acta* **1986**, *119*, 67.
(55) Reichert, C.; Bancroft, G. M.; Westmore, J. B. *Can. J. Chem.* **1970**, *48*, 1362.

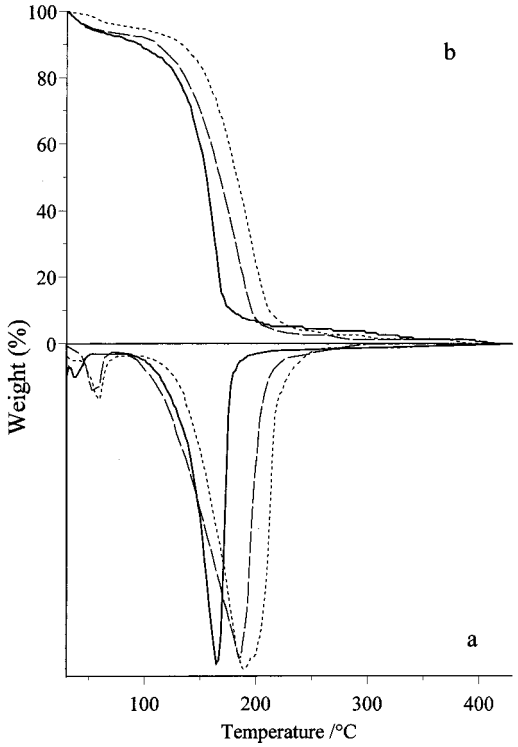

Figure 3. DTG (a) and TG (b) of $Zn(hfa)_2 \cdot 2H_2O \cdot$polyether adducts: solid lines refer to $Zn(hfa)_2 \cdot 2H_2O \cdot$diglyme, dashed lines refer to $Zn(hfa)_2 \cdot 2H_2O \cdot$triglyme, and dotted lines refer to $Zn(hfa)_2 \cdot 2H_2O \cdot$tetraglyme.

Table 3. DTG Analysis Temperatures (°C)

	precursors		
	1	2	3
1st peak	40.7	56.0	58.2
2nd peak	166.7	188.5	189.2

in agreement with those already observed for similar systems.[44,45]

TGA and DTG analyses of the $Zn(hfa)_2 \cdot 2H_2O \cdot$polyether adducts **1**−**3** all show two mass-loss processes in the 40−58 and 166−189 °C ranges (Figure 3 and Table 3). Lower temperature processes have associated a minor (≈5%) mass loss that, however, is nicely tuned with the following equation:

$$Zn(hfa)_2 \cdot 2H_2O \cdot \text{glyme} \rightarrow Zn(hfa)_2 \cdot \text{glyme} + 2H_2O \quad (1)$$

Similar dehydration temperatures have been reported for $Zn(hfa)_2 \cdot 2H_2O$[56] and $Zn(acac)_2 \cdot H_2O$.[57] The remaining 95% mass is lost quantitatively in the second step, almost without leaving residue (<1%) in all cases.

Figure 4 shows the DSC analysis of the prototypical $Zn(hfa)_2 \cdot 2H_2O \cdot$diglyme adduct. Two distinct endothermic peaks are observed at 37.2 (−109.3 kJ/mol) and 162.6 °C (−89.6 kJ/mol). They account for melting along with loss of coordinated water and evaporation from melt, respectively. The simultaneous occurrence of two processes renders the lower temperature peak much broader (ΔT = 14 °C) than that observed with other parent adducts[45] and the enthalpy value, associated with the whole process, somewhat larger.[45]

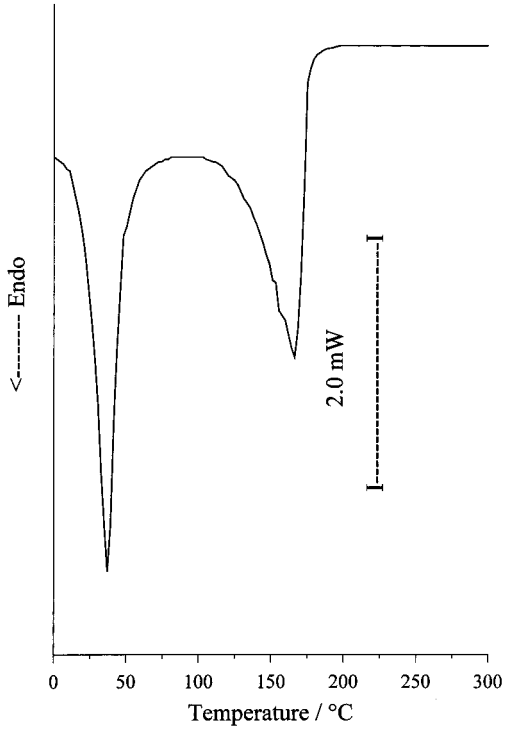

Figure 4. DSC curve of $Zn(hfa)_2 \cdot 2H_2O \cdot$diglyme.

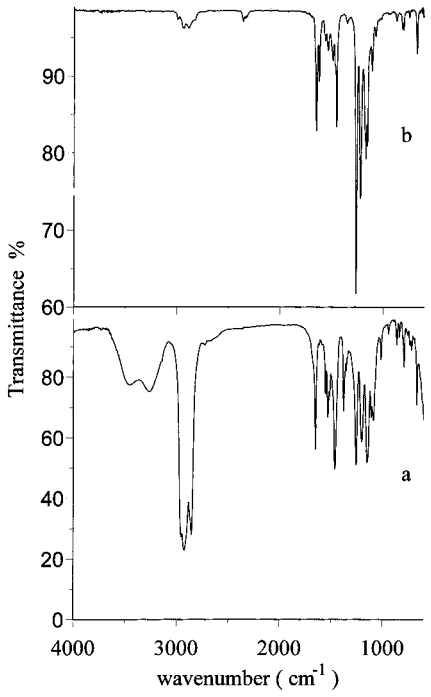

Figure 5. Prototypical IR spectra of **1**: (a) in Nujol mull; (b) gas phase.

Therefore, the lower temperature processes leave anhydrous, liquid adducts, which evaporate intact afterward. Identical conclusions can be arrived at by gas-phase IR data discussed in the following sections (vide infra).

The FT-IR transmittance spectra of solid **1** (Figure 5a), **2**, and **3** in Nujol mull show a broad envelope with two bumps in the 3450−3260 cm^{-1} range due to asymmetric and symmetric H_2O stretching modes, respectively.[58] In addition, bands at 1018−1022, 942−947, and 860−864 cm^{-1} can safely be associated with glyme

(56) Li, N. C.; Wang, S. M.; Walker, R. W. *J. Inorg. Nucl. Chem.* **1965**, *27*, 2263.
(57) Graddon, D. P.; Weeden, D. G. *Aust. J. Chem.* **1963**, *16*, 980.

modes.[44−45,59] Unfortunately, the C−H glyme stretching modes, lying in the 2800−3000 cm^{-1} range, overlap with Nujol IR features, thus precluding any further discussion.

It has been already reported that blueshifts ($\Delta \sim 10$ cm^{-1}) suffered by the 860 cm^{-1} IR band of the free diglyme represent sensible indications of the metal−glyme coordination.[44,59] The bands at 860−864 cm^{-1} in the present adducts appear only marginally shifted, thus providing indication of no direct bonding interaction with the Zn metal center.

The nature of vapors evaporating from melt has been investigated by low-pressure (10 Torr) gas-phase FT-IR experiments of the prototypical **1**. No sizable IR signals are detected up to 50 °C. Signals grow in the 55−150 °C temperature range and the resulting IR spectra are diagnostic of the anhydrous $Zn(hfa)_2$·diglyme adduct (Figure 5b). In fact, (i) there is no evidence of the H_2O stretching modes, (ii) the bands in the 2830−2998 cm^{-1} range are associated with the C−H (diglyme) stretching modes, and even more important, (iii) the relative ratios of absorbances associated with C−H diglyme modes (2830−2998 cm^{-1}) and the hfa C═O stretching (1648 cm^{-1}) remain strictly constant in the entire 55−150 °C temperature range. This observation, in addition, appears consistent with competing H_2O and diglyme ancillary ligation (eq 1) upon heating/melting in the 37−55 °C interval, the latter being favored in the melt.

Separate sublimation experiments in vacuo (10^{-2} Torr) of the white powders of **1**−**3** gave oils that returned to white solids upon air exposure. Their IR spectra are identical to those of the sources. The conclusion that emerges is again tuned with competition between water and polyether for metal coordination.

Prototypical MOCVD experiments have been carried out using the crude $Zn(hfa)_2$·$2H_2O$·diglyme adduct as a self-generating liquid Zn source. Evaporation rates suitable for MOCVD experiments (1.3−1.9 mg/min) have been found in the 70−80 °C range. The substrate temperature has been maintained in the 320−400 °C range, and the deposition time was 120−180 min.

XRD measurements (Figure 6) of as-deposited films provide evidence of hexagonal ZnO crystallites. The predominance of (002) and (101) reflections ($\theta = 34.49$ and 36.39, respectively) points to some texturing.[60] Interesting enough, fixed grazing-incident ($\theta = 0.5°$) XRD experiments show an increased intensity of the (002) reflection. It, therefore, turns out that the *c*-axis orientation is highly preferred in the topmost atomic layers of the ZnO films. Finally, the mean crystallite size evaluated from the XRD line broadening[51] (substrate temperature = 320 °C) is equal to 29.8 nm.

The deposited films are transparent, and their UV−visible spectra (Figure 7) find counterparts in previously reported data.[8,12,18,35,61−63] In particular, the transmittance has a minimum at $\lambda = 377$ nm (the absorption edge) and reaches a 90% value in the visible and near-infrared range.

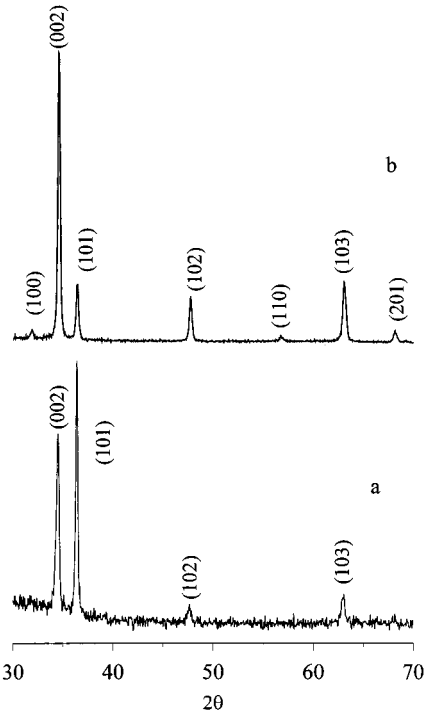

Figure 6. X-ray diffraction patterns, over a $30° < 2\theta < 70°$ angular range, for SiO_2-supported, ZnO as-deposited thin film: (a) $\theta-\theta$ and (b) grazing $\theta = 0.5°$.

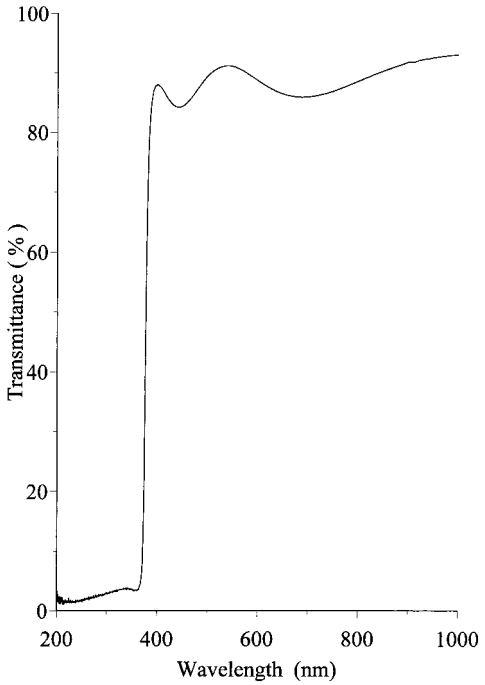

Figure 7. UV−visible transmission spectrum for a representative ZnO thin film on SiO_2 substrate.

(58) Morris, M. L.; Moshier, R. W.; Sievers, R. E. *Inorg. Chem.* **1963**, *2*, 411.
(59) Iwamoto, R. *Spectrochim. Acta* **1971**, *27A*, 2385.
(60) American Society for Testing and Material *Powder Diffraction Files*; Joint Committee on Powder Diffraction Standards; #3−888.
(61) Vispute, R. D.; Talyansky, V.; Sharma, R. P.; Choopun, S.; Downes, M.; Venkatesan, T.; Li, Y. X.; Salamanca-Riba, L. G.; Iliadis, A. A.; Jones, K. A.; McGarrity, J. *Appl. Surf. Sci.* **1998**, *127−129*, 431.
(62) Oktik, S.; Russell, G. J.; Brinkman, A. W. *J. Cryst. Growth* **1996**, *159*, 195.
(63) Warkm, M.; Kessler, H.; Schulz-Ekloff, G. *Microporous Mater.* **1997**, *8*, 241.

The film thickness d has been evaluated from UV−visible data using the classical equation:[64]

$$d = \frac{\lambda_1 \lambda_2}{2(\lambda_1 n_2 - \lambda_2 n_1)} \quad (2)$$

where n_1 and n_2 are the refractive indices at two adjacent maxima or minima at λ_1 and λ_2 wavelength. By assuming $n_1 = n_2 = 2.0$ for hexagonal ZnO films, the calculated d value is 380 nm for a 120 min experiment (source temperature = 70 °C). Therefore, the resulting growth rate of the ZnO film corresponds to ~32 Å/min.

Figure 8 shows relevant XPS data of the present ZnO films. The Zn 2p features (Figure 6a) consist of the main $2p_{3/2}$ and $2p_{1/2}$ spin−orbit components at 1021.4 and 1044.5 eV, respectively. The O 1s peak (Figure 6b) lies at 530.13 eV and shows a shoulder at 532.13 eV, possibly due to the presence of hydroxide species on the surface.[38,42,65] These features are identical to those already reported for related ZnO systems.[38,42,65] Photoemission spectra show, in addition, sizable features due to fluorine and carbon contaminants. In the C 1s region, three very weak signals at 284.6, 289.3, and 292.5 eV can be distinguished. The low binding energy signal is due to carbon contaminants being almost ubiquitous on all surfaces. The binding energies of the remainders as well as the band at 687.9 eV are likely to be due to C 1s and F 1s photoemitted electrons associated with CF_2/CF_3 groups adsorbed to the surface of the ZnO film.[38,66,67] This observation suggests the existence of some thermally activated side reactions associated with the precursor demolition on the substrate in the present operating conditions. In this context, XPS of Zn 2p, O 1s, F 1s, and C 1s peaks, taken at 45° emission relative to the surface plane, have been used to derive the effective surface composition of as-deposited films, making due allowance for the relevant atomic sensitivity factors.[67] It was found that the Zn/O intensity ratio is close to the expected 1:1 ratio, and quantitation of the C and F content gives values of 9 and 7% respectively. Further annealing experiments at 400 °C in air of films bring down the contaminants to less than 2%.

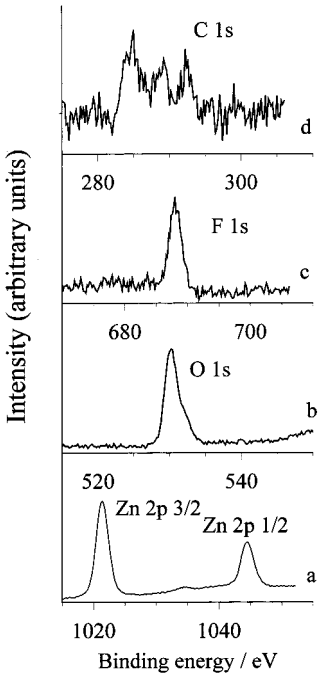

Figure 8. Al Kα excited XPS of a representative ZnO thin film measured in the (a) Zn 2p, (b) O 1s, (c) F 1s, and (d) C 1s energy regions. Structures due to satellite radiation have been subtracted from the spectra.

Conclusions

Three novel $Zn(hfa)_2 \cdot 2H_2O \cdot$polyether adducts have been synthesized with simple procedures. X-ray single-crystal data of the $Zn(hfa)_2 \cdot 2H_2O \cdot$diglyme show that H_2O is retained in the coordination array, whereas the polyether lies in the crystal with contact distances indicative of bridging hydrogen bonds. To our knowledge, this observation represents the first case of metal β-diketonates where glyme ligands do not favorably compete with H_2O. Interesting, mild heating experiments and gas-phase IR data show that dehydration can be thermally activated and that the anhydrous $Zn(hfa)_2 \cdot$ diglyme evaporates intact from melt/liquid.

Deposition experiments, in a low-pressure horizontal hot-wall reactor on fused SiO_2 substrates, result in ZnO thin films whose XRD spectra provide evidence that they are hexagonal and consist of (002) and (10*l*) oriented crystals. Optical spectra show that the transmittance of films is around 90% in the visible and near-IR range.

Acknowledgment. Drs. E. Amato, G. Condorelli, and G. Malandrino are gratefully acknowledged for NMR, gas-phase IR measurements, and availability of the MOCVD facility, respectively.

Supporting Information Available: Atomic coordinates, isotropic displacement parameters, bond lengths and angles, and structure factors. This material is available free of charge via the Internet at http://pubs.acs.org.

CM991154K

(64) Swanepoel, R. *J. Phys. E: Sci. Instrum.* **1983**, *16*, 1214.
(65) Schon, G. *J. Electron Spectrosc. Relat. Phenom.* **1973**, *2*, 75.
(66) Gelius, U.; Heden, P. F.; Hedman, J.; Lindberg, B. J.; Manne, R.; Nordberg, R.; Nordling, C.; Siegbahn, K. *Phys. Scr.* **1970**, *2*, 70.
(67) Wagner, C. D. *Practical Surface Analysis*, 2nd edition; Briggs, D., Seah, M. P., Eds., Wiley: Chichester, 1995; Appendix 5.